

High-Density Polyethylene Foams. I. Polymer and Foam Characterization

Yaolin Zhang, Denis Rodrigue, Abdellatif Ait-Kadi

Department of Chemical Engineering and Centre de Recherche en Science et Ingenierie de Macromolécules (CERSIM), Laval University, Quebec, Canada G1K 7P4

Received 18 September 2002; accepted 3 February 2003

ABSTRACT: The density and morphology of closed-cell high-density foams were investigated with four different molecular weights of high-density polyethylene (HDPE). The characterization of polyethylene via rheological methods was used to determine its influence on foam density and morphology. We found that foaming grade decreased with increasing molecular weight and increased with blowing agent content. The average cell size was also a strong function of molecular weight and blowing agent content. In-

creasing both the molecular weight and amount of blowing agent decreased the cell size. Cell size also increased for our lowest molecular weight HDPE but decreased for the others. Cell density also increased with increasing HDPE molecular weight. © 2003 Wiley Periodicals, Inc. *J Appl Polym Sci* 90: 2111–2119, 2003

Key words: density; polyethylene (PE); rheology; morphology

INTRODUCTION

Polyethylene (PE) foam is one of the most important plastic foams, and its commercial production started in the early 1940s.¹ Most polyolefin foams have a closed-cell structure, which makes them suitable for applications where buoyancy and insulation are important as well as resiliency for packaging applications. In addition, they are used in construction, transportation, sports and leisure, and agriculture. Since the 1940s, several studies focused on the processing mechanism,^{2–6} morphology, mechanical properties; the relationship between cell morphology and foam properties,^{7–14} and the effect of molecular structure on the cell morphology of PE foams.^{15–19}

However, much less work has been performed on the effect of molecular weight on the properties of high-density foams, including cell morphology and mechanical behavior. For this reason, we studied the rheological properties and the effect of molecular weight on the foaming process, morphology, and mechanical properties of high-density polyethylene (HDPE).

Traditional methods for molecular weight determination, such as light scattering, osmometry, and gel

permeation chromatography (GPC), require the polymer to be soluble in a solvent. Because PE does not dissolve in many solvents at room temperature, molecular weight measurements by light scattering and osmometry are difficult for PE because of the high temperature required. GPC measurement lacks sensitivity in the high-molecular-weight domain. It is not easy to measure high-molecular-weight HDPE with GPC, even at high temperatures. Therefore, many investigators have used intrinsic viscosity to estimate the molecular weight and have obtained different values, which were dependent on the correlation used. However, viscoelastic properties can be related to the polymer molecular weight and molecular weight distribution.^{20–26} It was found that the relationship between molecular weight and zero-shear viscosity (η_0) are hardly affected by polydispersity.²⁶

Abe and Yamaguchi¹⁵ investigated two low-density PEs with different chain branching. They found that the elastic modulus and crystallization temperature controlled the expansion ratio of crosslinked PE foams. As the elastic modulus increased, the expansion ratio of the foams decreased.

Yamaguchi and Suzuki¹⁶ studied the rheological properties and foam processability of PE blends and found that the addition of a small amount of crosslinked linear low-density PE enhanced the elongational viscosity and elastic properties, whereas it had little effect on the steady-state shear viscosity. The foams from these blends showed higher expansion ratios and more homogeneous cell size distributions.

Stafford et al.¹⁷ investigated polystyrene foams and suggested that molecular weight and polydispersity

Correspondence to: D. Rodrigue (denis.rodrigue@gch.ulaval.ca).

Contract grant sponsor: Natural Sciences and Engineering Research Council of Canada.

Contract grant sponsor: Fonds pour la Formation de Chercheurs et l'Aide à la Recherche of Quebec.

TABLE I
Raw Materials

HDPE	Melt index	Manufacturer
J60-1700-173	16.0 g/10 min ^a	Solvay Polymers
A60-70-162	0.72 g/10 min ^a	Solvay Polymers
G60-110	11.0 g/10 min ^b	Solvay Polymers
HBW555Ac	5.0 g/10 min ^b	Nova Chemicals

^a 190°C with 2.16 kg.

^b 190°C with 21.6 kg.

did not significantly affect the foaming process. However, low-molecular-weight fractions (<4%) had a great influence on the final structure of the foam and the cell diameter.

Chong et al.¹⁸ studied polyolefin foams processed by extrusion and observed that the degrees of foaming and cell sizes were related to the melt tension of the polymer, regardless of its structure, molecular weight, and melt temperature. For similar polymers, increasing the molecular weight simply increased the melt viscosity and reduced the foaming degree and cell size.

Xanthos et al.¹⁹ studied the foaming characteristics of poly(ethylene terephthalate) (PET). For medium-density and high-density foams, the important parameters affecting density were found to be the type and concentration of chemical blowing agent, the processing conditions, and to a certain extent, the resin viscosity. Foam density decreased with increasing intrinsic viscosity of the PET resin.

In this study, four different molecular weights of HDPE were used. The molecular weight was determined from rheological measurements, and its effect on cell morphology and foam density (ρ_f) is reported in this first article from the study.

EXPERIMENTAL

Polymer and sample preparation

Four HDPEs with different melt indices were used and are presented in Table I. J60-1700-173, A60-70-162, and G60-110 were homopolymers from Solvay Polymers Solvay Polymers (Houston, TX). HBW555-Ac was a high-molecular-weight PE from Nova Chemicals Nova Chemicals (Calgary, Alberta, Canada).

The foams were obtained by a compression-molding method. The PE-blowing agent compounds were blended with a laboratory internal mixer (Haake Rheomix, Karlsruhe, Germany) at 40–50 rpm and 150°C. The chemical blowing agent was azodicarbonamide (ACA; Sigma Chemicals, Milwaukee, WI), whose decomposition temperature range was 190–240°C and gas number was 230–270 cm³/g. Concentrations between 1 and 3% were used on the basis of the total weight of all of the components. In each

blend, 0.1% antioxidant, octadecyl-3,5-di-*tert*-butyl-4-hydroxyhydrocinnamate (Irganox 1076, Ciba-Geigy Corp., Hawthorne, NY), was added to prevent thermal oxidation during mixing and foam processes. The molding procedure was as follows:²⁷

1. The mold with the foamable compound was held at 150°C and 4.0 MPa for 10 min.
2. The mold was then heated at 200°C and the pressure was kept for 10 min.
3. After pressure removal, expansion took place immediately.
4. The foams were kept in the mold until they had been cooled down to 50°C with circulating water.

To investigate the rheological properties of the solid polymer, HDPE samples were also prepared without the blowing agent (unfoamed material).

Rheology measurements

Complex shear viscosity and moduli were measured with 25-mm diameter parallel plate geometry with 1-mm gaps via a Bohlin CVO HR 120 rheometer (East Brunswick, NJ). Strain sweep tests were first carried out to ensure that the tests were performed in the linear viscoelastic zone of each material before the frequency sweeps were performed.

Characterization of foams

Density

According to ASTM D 1622-98, the apparent density of foams was obtained by the ratio of the weight over the volume of each sample. The dimensions were measured with a micrometer, and the weights were carefully measured. The average apparent density was obtained by a minimum of two samples for each HDPE molecular weight and ACA concentration. The normalized density, which was defined as the ratio of the foamed to the unfoamed sample, was also determined.

Foaming grade

The foaming grade was determined by ρ_f and was calculated as:²⁸

$$\text{Foaming grade} = \left(1 - \frac{\rho_f}{\rho_m}\right) \times 100\% = V_f \times 100\% \quad (1)$$

where ρ_m is the density of the unfoamed polymer matrix and V_f is the volume fraction of voids.

Micrograph

Scanning electron microscopy (SEM) micrographs of the fractured surface of the foams were made at various magnifications. First, each specimen was placed under cryogenic conditions (liquid nitrogen) for more than 10 h to avoid damage to the surface morphology during cutting. Then, the specimens were cut with a Reichert-Jung 2050 microtome (Nussloch, Germany), and the cross-section of each specimen was coated with palladium. Finally, coated specimens were examined with a Jeol 840A scanning electron microscope (Tokyo, Japan).

Cell size

Quantitative image analysis was used to assess the cellular structure and measure the average cell size (D) with Image-Pro Plus image analysis software from Media Cybernetics (Silver Spring, MD). Each micrograph was analyzed with the following steps:

1. Tracing all the cells in the micrograph.
2. Calculating each cell's dimension with the software.
3. Averaging the mean cell diameter of all of the cells in the micrograph.

It was known that the average sphere diameter was larger than the average circular segment because the cells were randomly truncated with respect to the depth at the plane of the specimen fracture surface. We supposed that the foam consisted of randomly distributed cells with an identical diameter. D was determined with the following equation according to the appendix of ASTM D 3576:

$$D = d / (\pi/4) \quad (2)$$

where d is the measured average diameter in the micrograph.

Linear cell density (N_f) and cell density (N_0)

N_0 is defined as the number of cells nucleated per cubic centimeter of unfoamed polymer and is given by:^{28,29}

$$N_0 = \frac{N_f}{1 - V_f} \quad (3)$$

where N_f is the linear cell density (the cell number nucleated per cubic centimeter of the foam).²⁸

There were two options for calculating N_f . One was to count the number of cells in a SEM micrograph and to use the following equation:²⁸

$$N_f = \left(\frac{nM^2}{A} \right)^{3/2} \quad (4)$$

where n is the number of bubbles in the micrograph and A and M are the area and the magnification factor of the micrograph, respectively. Another method was to use the average cell diameter and ρ_f :

$$N_f = \frac{V_f}{\frac{\pi}{6} D^3} \quad (5)$$

RESULTS AND DISCUSSION

Polymer characteristics

For polymers with molecular weights higher than their critical molecular weight, the relationship between weight-average molecular weight (M_w) and η_0 is^{20,26}

$$\eta_0 = kM_w^\alpha \quad (6)$$

where k is a constant specific for each type of polymer and α is around 3.2–3.6 for linear polymers.

Master curve for HDPE

It is known that the rheology of polymer melts depends strongly on temperature. Isotherms of the storage modulus [$G'(\omega)$] and isotherms of the loss modulus [$G''(\omega)$] can be superimposed by horizontal shifts along the frequency axis (ω) via the time-temperature superposition principle as

$$G^{(*)}(\omega a_T, T_0) = G^{(*)}(\omega, T) \quad (7)$$

where a_T is the temperature shift factor and T_0 is the reference temperature.

The temperature dependence of the shift factor follows an Arrhenius equation:²⁰

$$a_T = \exp \left[\frac{\Delta H}{R} \left(\frac{1}{T} - \frac{1}{T_0} \right) \right] \quad (8)$$

where ΔH is the activation energy for flow, R is the universal gas constant, and T is the testing temperature. The master curves for HDPE complex viscosity [$\eta^* = \omega^{-1}(G'^2 + G''^2)^{1/2}$], where G' is the storage modulus and G'' is the loss modulus, as a function of frequency are presented in Figure 1 for a T_0 of 200°C. The viscosity of HDPE increased in the following order: J60-1700-173 < A60-70-162 < G60-110 < HBW555Ac.

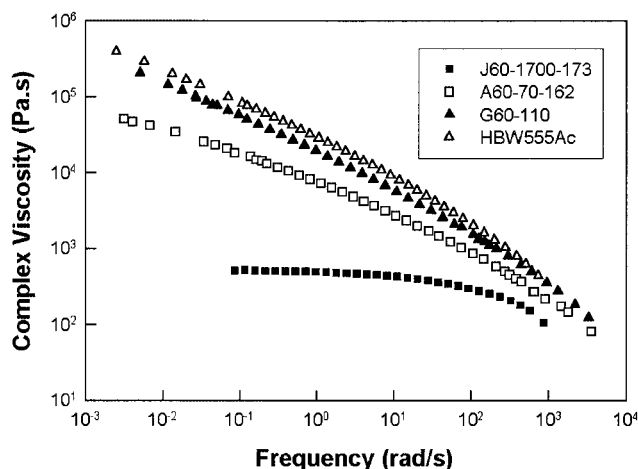


Figure 1 Master curves for η^* as a function of frequency at 200°C.

η_0

Typical dynamic mechanical data are different for low- and high-molecular-weight polymers. The dynamic viscosity for the low-molecular-weight polymer reaches a constant value at low frequencies, which is the η_0 . However, this value for high-molecular-weight materials is difficult to obtain directly because of experimental limitations (rheometer sensibility, long experimental time, possible degradation, etc.). As shown in Figure 1, η_0 could not be obtained directly from the viscosity curves, except for that of J60-1700-173. For the other HDPEs, some approximations were used to estimate the η_0 from the dynamic mechanical spectrum.^{20–21}

η_0 via G''

The real component ($\eta' = G''/\omega$) of the dynamic viscosity (η^*) for viscoelastic liquids reaches the η_0 as the frequency approaches zero. This means that

$$\eta_0 = \lim_{\omega \rightarrow 0} \frac{G''}{\omega} \quad (9)$$

For this equation to work, it is necessary to obtain the limiting straight-line behavior at low frequency (terminal zone). In this case, it is easy to read the η_0 from the curve of viscosity as function of frequency. This equation cannot be used when G''/ω does not yield a constant value.

In our study, the G''/ω of J60-1700-173 yielded constant value at low frequency; the value was about 516 Pa · s at 200°C, equivalent to about 570 Pa · s at 190°C. However, the G''/ω data for the other three samples did not reach a constant value; therefore, this method could not be used.

η_0 via G' (relaxation spectrum)

For uncrosslinked polymers, there is a relationship between the η_0 and dynamic modulus as

$$\eta_0 = \frac{2}{\pi} \int \frac{G'}{\omega} d \ln \omega \quad (10)$$

For eq. (10) to work, it is necessary to obtain the entire dynamic mechanical spectrum. The relation can be converted with the relaxation spectra based on the infinite Maxwell model²⁰ as

$$\eta_0 = \int_{-\infty}^{+\infty} \tau H(\tau) d \ln \tau \quad (11)$$

where τ is the relaxation time and $H(\tau) d \ln \tau$ is the relaxation spectrum. Grandjean et al.²⁵ developed a computer software to calculate the η_0 on the basis of eq. (11) with the modulus decomposition and the assumption that the curve of $H(\tau)$ as a function of $\ln \tau$ is symmetrical. Extrapolation at low frequency was thus needed because of experimental limitations of the rheometers:

$$G'(\omega) = \int \frac{\omega^2 \tau^2}{1 + \omega^2 \tau^2} H(\tau) d(\ln \tau) \quad (12)$$

$$G''(\omega) = \int \frac{\omega \tau}{1 + \omega^2 \tau^2} H(\tau) d(\ln \tau) \quad (13)$$

From dynamic measurements, the η_0 was obtained with this software, and the η_0 results are listed in Table II.

η_0 from the Cole–Cole plot

η^* of various molten entangled polymers as a function of frequency can be decomposed into its real and imaginary parts as

$$\eta^*(\omega) = \eta'(\omega) - i\eta''(\omega) \quad (14)$$

TABLE II
 η_0 of HDPE at 190°C

HDPE	Method 1	Method 2	Average
J60-1700-173	5.55×10^2	5.77×10^2	5.66×10^2
A60-70-162	2.54×10^5	1.63×10^5	2.08×10^5
G60-110	2.61×10^6	2.46×10^6	2.57×10^6
HBW555Ac	4.68×10^6	3.50×10^6	4.09×10^6

Method 1: computer software; Method 2: Cole–Cole plot.

TABLE III
Molecular Weight of HDPE

HDPE	Method 1	Method 2	Average
J60-1700-173	6.04×10^4	5.61×10^4	5.83×10^4
A60-70-162	3.31×10^5	3.19×10^5	3.25×10^5
G60-110	6.33×10^5	6.68×10^5	6.51×10^5
HBW555Ac	7.45×10^5	7.66×10^5	7.56×10^5

Method 1: Raju's equation; Method 2: Yamamoto and Furukawa's equation.

where $\eta^*(\omega)$, $\eta'(\omega)$, and $\eta''(\omega)$ are the complex viscosity and the real and imaginary parts of the complex viscosity, respectively, and i is the imaginary unit (the square root of -1). The components of η^* are related to G' and G'' by

$$\eta' = G'' / \omega, \quad \eta'' = G' / \omega \quad (15)$$

In the early 1970s, Labaig and coworkers^{30,31} reported a simple empirical method for analyzing the dynamic rheological data of molten polymers. They proposed the use of the Cole-Cole analytic expression^{32,33} to represent the η^* of polymers in the low-frequency range:

$$\eta^*(\omega) = \frac{\eta_0}{1 + (i\omega\lambda_0)^{1-\beta}} \quad (16)$$

where λ_0 is the characteristic relaxation time corresponding to the frequency (ω_c) when η'' is maximum ($\lambda_0 = 1/\omega_c$) and β is a coefficient such that $(\pi\beta)/2$ is defined as the angle between the diameter through the origin of the circular arc and the real axis, of which the value is between 0 and 1. Equation (16) can be rewritten as

$$\left(\eta' - \frac{\eta_0}{2}\right)^2 + \left[\eta'' + \tan\left(\frac{\pi}{2}\beta\right)\frac{\eta_0}{2}\right]^2 = \left[\frac{\eta_0}{2\cos(\pi\beta/2)}\right]^2 \quad (17)$$

Lanfray and Marin³⁴ and Vega et al.³⁵ adopted this method for the analysis of the dynamic properties of PE melts. With this method, it was possible to get a good approximation of the η_0 for high-molecular-weight HDPEs. The results are listed in Table II for comparison. For the lowest molecular weight (J60-1700-173) HDPE, the η_0 values obtained from both methods were similar, but for other HDPEs, some differences were observed. Because both methods are

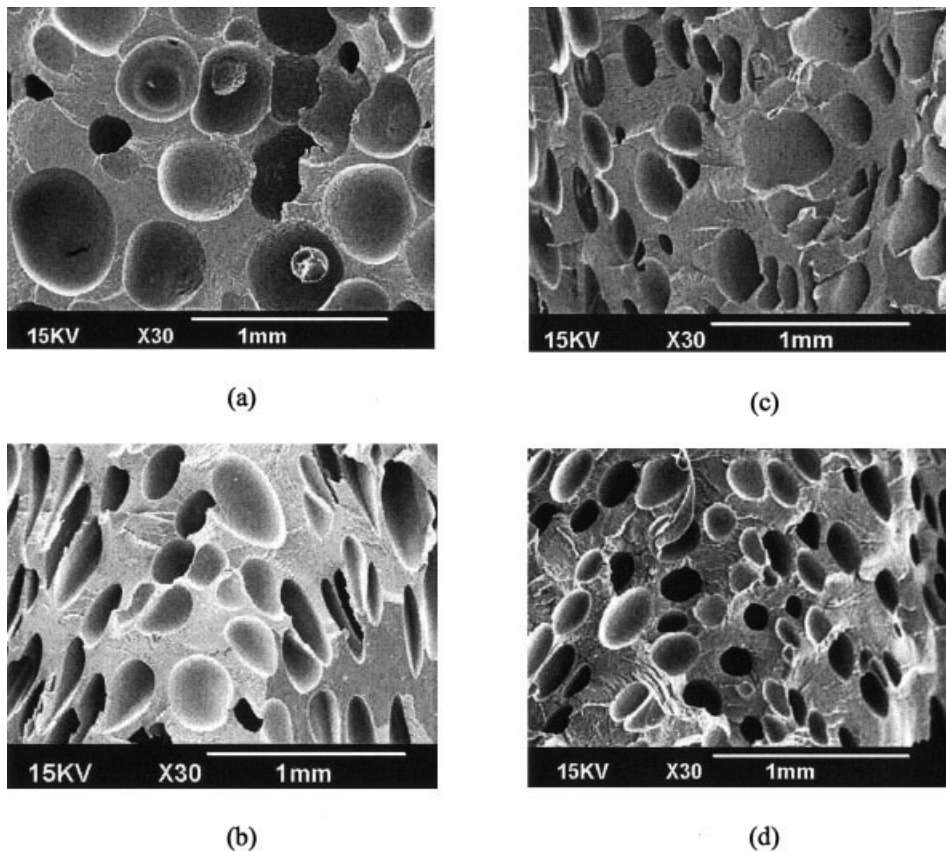


Figure 2 SEM micrographs of HDPE foams with 2% ACA: (a) J60-1700-173 (0.588 g/cm³), (b) A60-70-162 (0.569 g/cm³), (c) G60-110 (0.591 g/cm³), and (d) HBW555Ac (0.687 g/cm³).

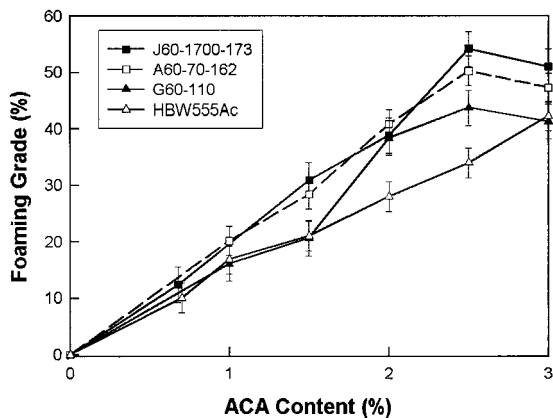


Figure 3 Foaming grade as a function of ACA content.

based on different assumptions for high-molecular-weight HDPE and because of experimental errors and rheometer limitations, the average value of η_0 was used in our calculations.

Molecular weight

When η_0 is known, eq. (6) can be used to calculate the molecular weight if the parameters k and α are known. Raju et al.³⁶ proposed a relationship between the value of η_0 at 190°C and M_w for PE as

$$\eta_0 = 3.4 \times 10^{-15} M_w^{3.60} \quad (18)$$

Yamamoto and Furukawa³⁷ proposed another equation based on the free volume of the polymer:

$$\log \eta_0 = \log\left(\frac{N_A}{6}\right) + \log\left(\frac{C_\infty^3 \langle l_v^2 \rangle}{m_v}\right) + 3.4 \log\left(\frac{M_w}{2M_e}\right) + \log \xi(\rho) \quad (19a)$$

$$\log \xi(\rho) = -10.6 + \frac{1}{2.303 f_g + \alpha_f(T - T_g)} \quad (19b)$$

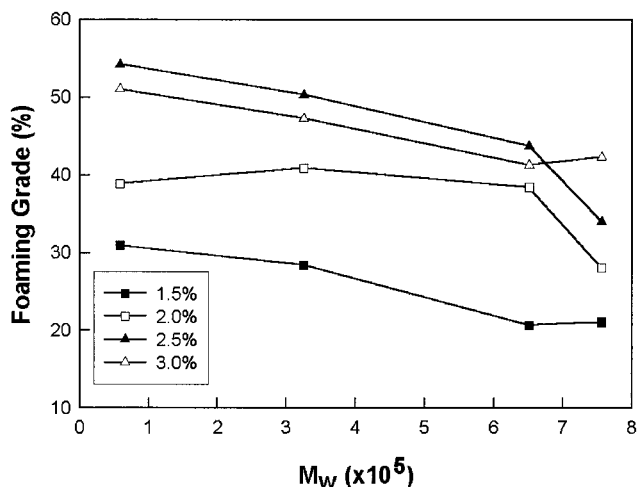


Figure 4 Foaming grade as a function of M_w for different ACA concentrations.

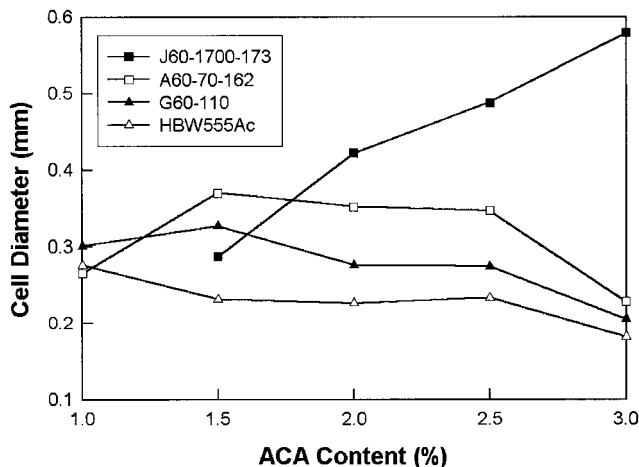


Figure 5 Average cell diameter as a function of ACA content.

where N_A is Avogadro’s number, C_∞ is the characteristic ratio, $\langle l_v^2 \rangle$ is the mean square length of the statistical skeletal bond, m_v is the molecular weight of the statistical skeletal bond, M_e is the entangled molecular weight of polymer, ξ is the free-volume function, f_g is the free-volume fraction at the glass-transition temperature, and α_f is the thermal expansion coefficient. For PE, eq. (19a) can be rewritten as

$$\eta_0 = 4.032 \times 10^{-14} M_w^{3.4} \quad \text{at } 190^\circ\text{C} \quad (20)$$

to calculate M_w when η_0 is known. The results are listed in Table III. Differences in the values from both methods were small. The average value of the molecular weight was used.

Foam morphology

Cell structure

Typical SEM micrographs of the foams are shown in Figure 2. It is known that HDPE foams usually have

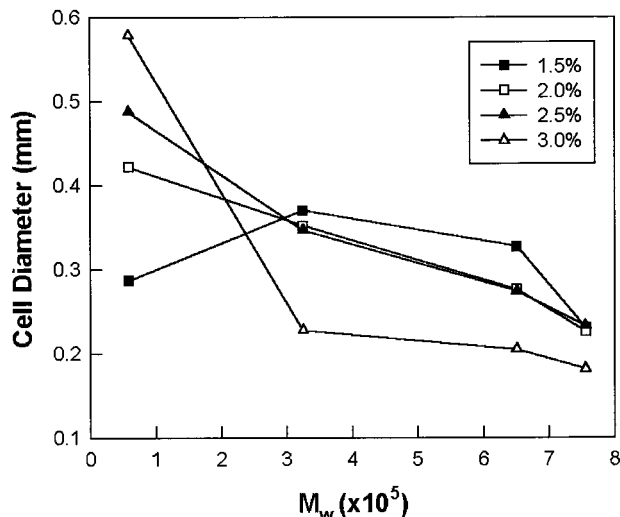


Figure 6 Average cell diameter as a function of M_w .

TABLE IV
 N_0 as a Function of ACA Concentration

ACA (%)	N_0 (cells/cm ³)							
	J60-1700-173		A60-70-162		G60-110		HBW555Ac	
	Eq. (3) and (4)	Eq. (3) and (5)	Eq. (3) and (4)	Eq. (3) and (5)	Eq. (3) and (4)	Eq. (3) and (5)	Eq. (3) and (4)	Eq. (3) and (5)
1.0	—	—	2.02×10^4	2.57×10^4	1.76×10^4	1.36×10^4	2.72×10^4	2.07×10^4
1.5	3.09×10^4	3.61×10^4	2.16×10^4	1.48×10^4	2.32×10^4	1.44×10^4	4.44×10^4	4.15×10^4
2.0	1.55×10^4	1.62×10^4	3.06×10^4	3.01×10^4	4.93×10^4	5.69×10^4	7.93×10^4	6.46×10^4
2.5	1.47×10^4	1.94×10^4	3.14×10^4	4.60×10^4	5.87×10^4	7.23×10^4	7.79×10^4	7.74×10^4
3.0	9.29×10^3	1.03×10^4	2.00×10^5	1.43×10^5	1.70×10^5	1.57×10^5	2.10×10^5	2.31×10^5

closed-cell structures. As shown in Figure 2, all of our HDPE foams seemed to have a closed-cell structure. Increasing the molecular weight seemed to give smaller cell sizes, which could have been related to their higher viscosity. A higher viscosity generally implies a higher resistance to foaming and a smaller cell size.

Effect of ACA content on the foaming grade

The effect of ACA content on the foaming grade is shown in Figure 3. Increasing the blowing agent concentration up to 2.5% increased the foaming grade, where it reached a plateau, except for the highest molecular weight HDPE foam. The amount of gas available for foaming was directly related to the concentration of the blowing agent. Generally speaking, the foaming grade increased with ACA content if all the gas produced by ACA decomposition stayed in the polymer. As shown in a previous study,³⁸ the ratios of melt elongational viscosity over melt shear viscosity had similar shapes for these HDPEs. This means that these PEs had similar stress-hardening behaviors. The only difference was their viscosity. For different molecular weights, increasing the molecular weight increased the viscosity of the melt polymer, as

shown in Figure 1. For very high molecular weights, the forces associated with gas expansion in the bubbles were not strong enough to overcome the resistance because of the higher viscosity, and the foaming grade of the high-molecular-weight HDPE was lower than that of the low-molecular-weight HDPE at the same ACA content. As seen in Figure 4, the foaming grade of PE foams had the following trend: HBW555AC < G60-110 < A60-70 < J60-110.

The smaller expansion ratio resulted from the higher viscosity and the larger resistance of bubble growth along with the higher molecular weight. These results are in agreement with Chong et al.¹⁸ for extruded polyolefin foams.

Because the solubility of a gas in a polymer at high temperature is limited, a surplus amount of ACA could not produce a higher foaming grade because the diffusion loss of gas limited the efficiency of the blowing agent. There was competition between the diffusion and the resistance of viscosity. For ACA concentrations higher than 2.5%, a diffusion loss of gas was believed to occur for J60-1700-173, A60-70-162, and G60-110. However, for the highest molecular weight HDPE (HBW555AC), the diffusion loss of gas from the

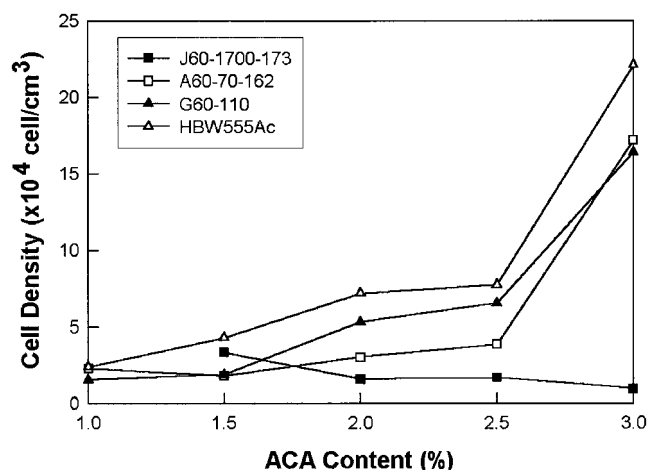


Figure 7 N_0 as a function of ACA content.

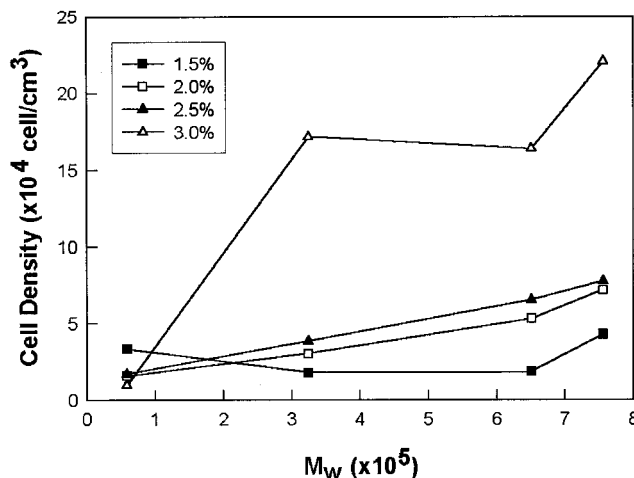


Figure 8 N_0 as a function of M_w for different ACA concentrations.

polymer may have been prevented because of the high resistance of the viscosity producing a higher internal cell pressure.

Cell size

As expected, the dimensions of the cells in the foam were a strong function of the blowing agent concentration and the polymer molecular weight. The variation of cell size with ACA concentration is shown in Figure 5. The effect of molecular weight on cell size is shown in Figure 6.

There are two fundamental steps in the determination of the cellular structure in a molten polymer saturated with gas: nucleation and growth. For a given foam volume, the system will be more stable with fewer large cells than with several smaller cells. This energy minimization factor favors cell coalescence. At 200°C, the viscosity of J60-1700 was lowest, followed by A60-70 and G60-110. That of HBW555Ac was the highest. Therefore, to reach a dynamical stability, smaller bubbles tended to combine into bigger bubbles. The lower the viscosity of the polymer melts was, the easier cell could combination occur. Because of its low viscosity, this kind of cell combination was the easiest for J60-1700. This explained the steeper increase in the average cell diameter for J60-1700 foams than for other foams as the concentration of ACA increased. However, because of the high viscosity of high-molecular-weight PE, the forces for gas expansion in the bubbles were not strong enough to overcome the resistance; thus, the coalescence of cells was very difficult. As the amount of blowing agent increased, the degree of foaming increased. At that time, the number of gas bubbles increased with initial nucleation. The final size of the gas bubbles was determined by a competition between coalescence, resistance of viscosity, and number of initial bubbles from nucleation. As molecular weight increased, the cell size first increased with ACA content, reached an optimum, and then decreased because of a greater number of initial bubbles from nucleation and some gas loss for G60-110 and A60-70-162 for ACA contents more than 2.5%. For the highest molecular weight, the cell size decreased along with ACA content.

N_0

The values of N_0 determined by two methods are presented in Table IV. The differences in the values obtained by both methods were small, and the average value was adopted to show the effect of ACA content in Figure 7. The N_0 of the lowest molecular weight HDPE foam decreased with increasing ACA concentration, but for high-molecular-weight PEs, the N_0 first increased with increasing ACA concentration and, at a critical concentration, reached a level and then in-

creased rapidly. The effect of molecular weight on N_0 is shown in Figure 8. Increasing molecular weight resulted in an increase in N_0 . Because resistance to bubble growth was very high for these high-viscosity polymers, it probably required less energy to create a new bubble by nucleation than to inflate an existing one by diffusion and mass transfer.

CONCLUSIONS

The molecular properties of different HDPEs were first investigated. The molecular weights of the HDPEs were calculated with rheological methods. Then, the morphology of the HDPE foams was investigated to determine the effect on ρ_f and morphology. Several conclusions were obtained by analysis of the data:

1. All HDPE foams with different molecular weights had closed-cell structures.
2. Foaming grade was strongly dependent on ACA concentration and the polymer matrix. The obtained foaming grades were proportional to ACA concentrations lower than 2.5%. A plateau was observed for ACA contents higher than 2.5%, except for the highest molecular weight HDPE. Increasing the molecular weight resulted in a decrease in the foaming grade.
3. Foam cell sizes were also strong functions of the molecular structure and ACA concentration. For the lowest molecular weight HDPE, the cell size increased as ACA concentration increased. As molecular weight increased, cell size first increased with ACA content, then reached a maximum, and decreased. For the highest molecular weight HDPE, cell size only decreased with ACA content because of high resistance (viscosity).
4. N_0 was a strong function of molecular weight and blowing agent concentration. For the lowest molecular weight structure HDPE, the N_0 decreased with ACA concentration. For high-molecular-weight HDPE, the N_0 increased with ACA concentration. Clearly, increasing the molecular weight resulted in an increase in N_0 .

The authors thank James M. Killough of BP Solvay Polyethylene North America Technical Center and Sarah Marshall of Nova Chemicals for the HDPE samples used in this study. They also want to mention the tragic loss of one the authors (A.A.-K.) to a car accident in the course of this study.

References

1. Burillo, G.; Adem, E. In *Polymeric Materials Encyclopedia*; CRC: Boca Raton, FL, 1996; Vol. 8.

2. Blyler, L. L., Jr.; Kwei, T. K. *J Polym Sci Part C: Polym Symp* 1971, 35, 165.
3. Donald, M. B.; Joseph, R. P. *Polym Eng Sci* 1976, 16, 706.
4. Kraynik, A. M. *Polym Eng Sci* 1980, 21, 80.
5. Han, C. D.; Villamizar, C. A. *Polym Eng Sci* 1978, 18, 669.
6. Han, C. D.; Ma, C. Y. *J Appl Polym Sci* 1983, 28, 831.
7. Gent, A. N.; Thomas, A. G. *Rubber Chem Technol* 1963, 36, 597.
8. Dutta, A.; Cakmak, M. *Rubber Chem Technol* 1993, 65, 933.
9. Throne, J. L. In *Engineering Guide to Structural Foams*; Wendle, B. C., Ed.; Technomic: Westport, CT, 1976.
10. Mehta, B. S.; Colombo, E. A. *J Cell Plast* 1976, 12, 59.
11. Wasserstrass, J. D.; Throne, J. L. *J Cell Plast* 1976, 12, 98.
12. Gonzalez, H. *J Cell Plast* 1976, 12, 49.
13. Hobbs, S. Y. *J Cell Plast* 1976, 12, 258.
14. Shutov, F. A. *Integral/Structural Polymer Foams: Technology Properties and Applications*; Springer-Verlag: Berlin, 1986.
15. Abe, S.; Yamaguchi, M. *J Appl Polym Sci* 2001, 79, 2146.
16. Yamaguchi, M.; Suzuki, K.-I. *J Polym Sci Part B: Polym Phys* 2001, 39, 2159.
17. Stafford, C. M.; Russel, T. P.; McCarthy, T. J. *Polym Prepr* 1999, 40, 551.
18. Chong, H. L.; Lee, K.; Ho, G. J.; Seong, W. K. *Adv Polym Technol* 2000, 19, 97.
19. Xanthos, M.; Zhang, Q.; Dey, A. S.; Li, Y.; Yilmazer, U.; O'Shea, M. *J Cell Plast* 1998, 34, 498.
20. Ferry, J. D. *Viscoelastic Properties of Polymers*, 3rd ed.; Wiley: New York, 1980.
21. Bird, R. B.; Armstrong, R. C.; Hassager, O. *Dynamics of Polymeric Liquids*, 2nd ed.; Wiley: New York, 1987; Vol. 1.
22. Yu, T. L. *J Macromol Sci Phys* 1992, 31, 175.
23. Fetters, L. J.; Lohse, D. J.; Richter, D.; Witten, T. A.; Zirkel, A. *Macromolecules* 1994, 27, 4639.
24. Machado, M. A. L.; Biagiotti, J.; Kenny, J. M. *J Appl Polym Sci* 2001, 81, 1.
25. Grandjean, B. P. A.; Ait-Kadi, A.; Côté, M. Presented at the Second International Symposium on Neural Computation, Berlin, May 23–26, 2000.
26. Gahleitner, M. *Prog Polym Sci* 2001, 26, 895.
27. Zhang, Y.; Rodrigue, D.; Zhang, Z.; Ait-Kadi, A. In *PPS-17 Conference Proceedings*, Montreal, Canada; Canadian Society of Rheology: Montreal, Canada, May 21–24, 2001; Paper 269.
28. Huang, Q.; Klötzer, R.; Seibig, B.; Paul, D. *J Appl Polym Sci* 1998, 69, 1753.
29. Matuana, L. M.; Park, C. B.; Balatinecz, J. T. *Polym Eng Sci* 1997, 37, 1137.
30. Labaig, J. J.; Monge, P.; Bednarick, J. *Polymer* 1973, 14, 384.
31. Marin, G.; Labaig, J. J.; Monge, P. *Polymer* 1975, 16, 223.
32. Cole, K. S.; Cole, R. H. *J Chem Phys* 1941, 9, 341.
33. Cole, K. S.; Cole, R. H. *J Chem Phys* 1942, 10, 98.
34. Lanfray, Y.; Marin, G. *Rheol Acta* 1990, 29, 390.
35. Vega, J. F.; Fernandez, M.; Santamaria, A.; Munoz-Escalona, A.; Lafuente, P. *Macromol Chem Phys* 1999, 200, 2257.
36. Raju, V. R.; Smith, G. G.; Marin, G.; Knox, J. R.; Graessley, W. W. *J Polym Sci Phys Ed* 1979, 17, 1183.
37. Yamamoto, T.; Furukawa, H. *J Appl Polym Sci* 2001, 80, 1609.
38. Zhang, Y.; Rodrigue, D.; Ait-Kadi, A. *Soc Plast Eng Annu Tech Conf Tech Pap* 218; Society of Plastics Engineers: Brookfield, CT, 2002.